The REME Phases

I. An Overview of Their Structural Variety

by **Mihaela D. Bojin** and **Roald Hoffmann***

Department of Chemistry and Chemical Biology, Cornell University, Ithaca, New York 14853-1301, USA
(e-mail: rh34@cornell.edu)

Dedicated to Professor *Jack D. Dunitz*, who thinks more deeply about structure than anyone else we know

There are more than 2000 compounds with RE/M/E 1:1:1 stoichiometry, where RE is a rare earth, actinide, or from groups 1–4, E is a late transition metal from groups 8–12, and E belongs to groups 13–15. In the first paper of a series, we describe the primary structural characteristics of this large class of compounds, focusing on the geometries and bonding in the $[ME]^{n-}$ anionic sublattices. We start with a detailed description of the EuAuSn lattice, by emphasizing its essential building blocks and the symmetry operations connecting them, in order to set up a way of describing systematically the geometric features of other REME frameworks. Nearly all these phases have eclipsed hexagonal layered arrangements (with only M–E bonds within these slabs) in the ME sublattice. In most cases, stacking the puckered layers in the third dimension gives rise to M–E, M–M, or E–E bonds, alternating in certain patterns. We point to several interesting sets of REME compounds, of like structure, but whose electron counts vary significantly. The structures of nonlayered networks and their most-common electron counts are also introduced.

Enumeration. – In this work, we begin to look at bonding patterns in a large group of ternary compounds with the RE/M/E 1:1:1 stoichiometry, where RE = rare earth (lanthanide (Ln) or actinide (An)), alkali, alkaline earth, or from groups 3 and 4, M = late transition metal, from groups 8–12, and E = main group element, from groups 13–15. In the periodic table in *Fig. 1*, we highlighted with yellow the elements we refer to as RE, M in red, and E in blue. We will call the general class the REME structures. In CRYSTMET (a database for inorganic compounds) [1] and ICSD (Inorganic Crystal Structure Database) [2], more than 2000 substances fall into this category.

As shown in *Table 1*, more than 60% of compounds have a lanthanide (Ln) as countercation. This is the reason for our use of RE in the REME class notation, albeit many phases do not contain a lanthanide. In *Tables 2* and *3* from *Appendix*, we list the compounds, grouping them (somewhat arbitrarily) by the space groups in which they crystallize, and give the archetypical structure types, along with simple descriptions of their structural characteristics and electron counts. We are going to refer to these tables throughout our subsequent discussion.

We abbreviate orthorhombic-REME as o-REME, hexagonal-REME as h-REME, cubic-REME as c-REME, tetragonal-REME as t4-REME, trigonal-REME as t3-REME, and monoclinic-REME as m-REME.

As may be seen from *Table 1*, there is – to put it mildly – a myriad of REME phases, covering most but not all possibilities.

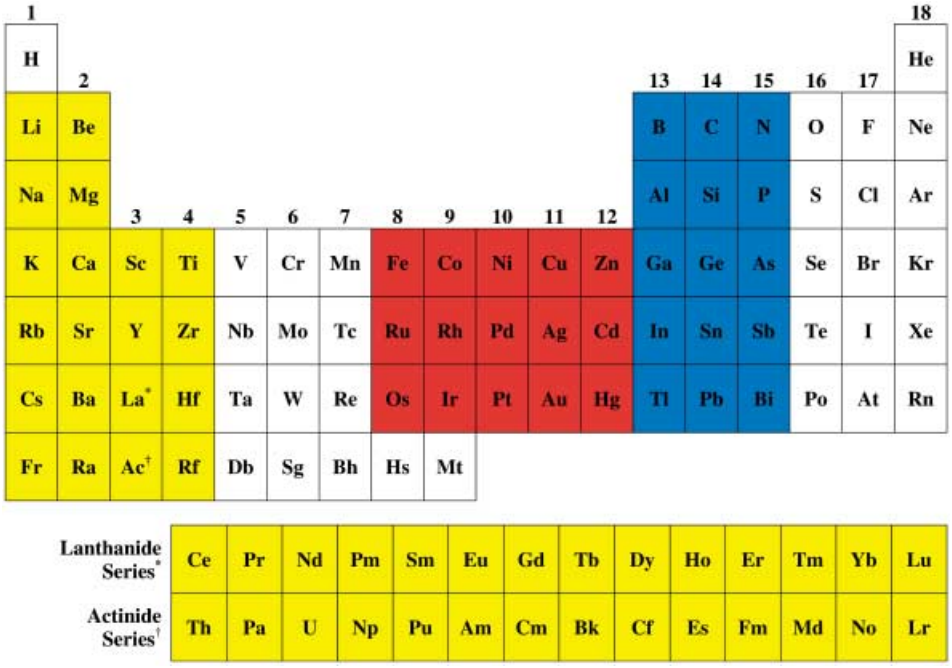

Fig. 1. *In this periodic table, the elements we label RE are highlighted in yellow, M in red, and E in blue*

A Typical (Complicated) REME Structure: EuAuSn. – To sample the structural richness of this class of composites and to broach the problems posed by it, let's start by examining an illustrative, not simplest, representative. EuAuSn, synthesized by *Pöttgen et al.* [3], is a paradigm for the orthorhombic REMEs (o-REMEs). The structure is shown in *Fig. 2*.

EuAuSn has an intricate framework, containing in the unit cell no fewer than ten formula units. Underlying this complexity, however, are some rather simple building blocks and a layering principle.

Eu–Au or Eu–Sn distances in EuAuSn are in the range of normal or weak ionic interactions (greater than 3.3–3.4 Å for both types, between 125–150% of the sums of covalent or ionic radii; $r_{Eu^{2+}} = 1.17$ Å, $r_{Au^{+}} = 1.37$ Å, $r_{Au^{0}} = 1.34$ Å, $r_{Sn^{0}} = 1.40$ Å). Hence, as a first simplification, we omit the Eu-atoms from consideration. The magnetic measurements carried out on EuAuSn indicate that the Eu's oxidation state is $+2$. We then assume that the remnant polyanionic network, on which we will concentrate in our study, bears a -2 charge, $[AuSn]^{2-}$. Further, if we count the electrons in a *Zintl* way, and assign to Au a $+1$ charge, (considering its coordination environments, distorted tetrahedral and trigonal planar), then Sn has to bear three electrons, as Sn^{3-}. Such an ion is prone to form dimers, thus Sn–Sn bonds should be present in the structure. By analyzing the $[AuSn]^{2-}$ sublattice, one notes that indeed there are a number of such dimers. Nevertheless, a large proportion of the Sn's form exclusively Au–Sn bonds.

Table 1. *The Number of REMEs, Depending on the Identity of RE, M, and E*. The entries in the RE, M, and E columns are groups of the periodic table. For example, in the (1)(8–10)(13) series – RE in group 1, M in groups 8–10, and E in group 13 – there are 10 ternaries with a 1:1:1 stoichiometry. Overall, we found 2063 REME compounds. Tomorrow, there will be more.

RE	M	E	Σ(E)	Σ(M)	Σ(RE)	Sum REME
1	8–10	13	10	13	*43*	2063
		14	0			
		15	3			
	11	13	1	4		
		14	2			
		15	1			
	12	13	0	26		
		14	1			
		15	25			
2	8–10	13	6	60	*121*	
		14	23			
		15	31			
	1	13	8	60		
		14	9			
		15	43			
	12	13	0	1		
		14	1			
		15	0			
3	8–10	13	38	160	*221*	
		14	96			
		15	26			
	11	13	14	52		
		14	38			
		15	0			
	12	13	8	9		
		14	1			
		15	0			
4	8–10	13	30	190	*214*	
		14	94			
		15	66			
	11	13	10	23		
		14	13			
		15	1			
	12	13	1	1		
		14	0			
		15	0			
An	8–10	13	80	157	*179*	
		14	68			
		15	9			
	11	13	9	22		
		14	13			
		15	0			
	12	13	0	0		
		14	0			
		15	0			
Ln	8–10	13	273	870	*1285*	
		14	435			
		15	162			
	11	13	131	334		
		14	182			
		15	21			
	12	13	50	81		
		14	31			
		15	0			

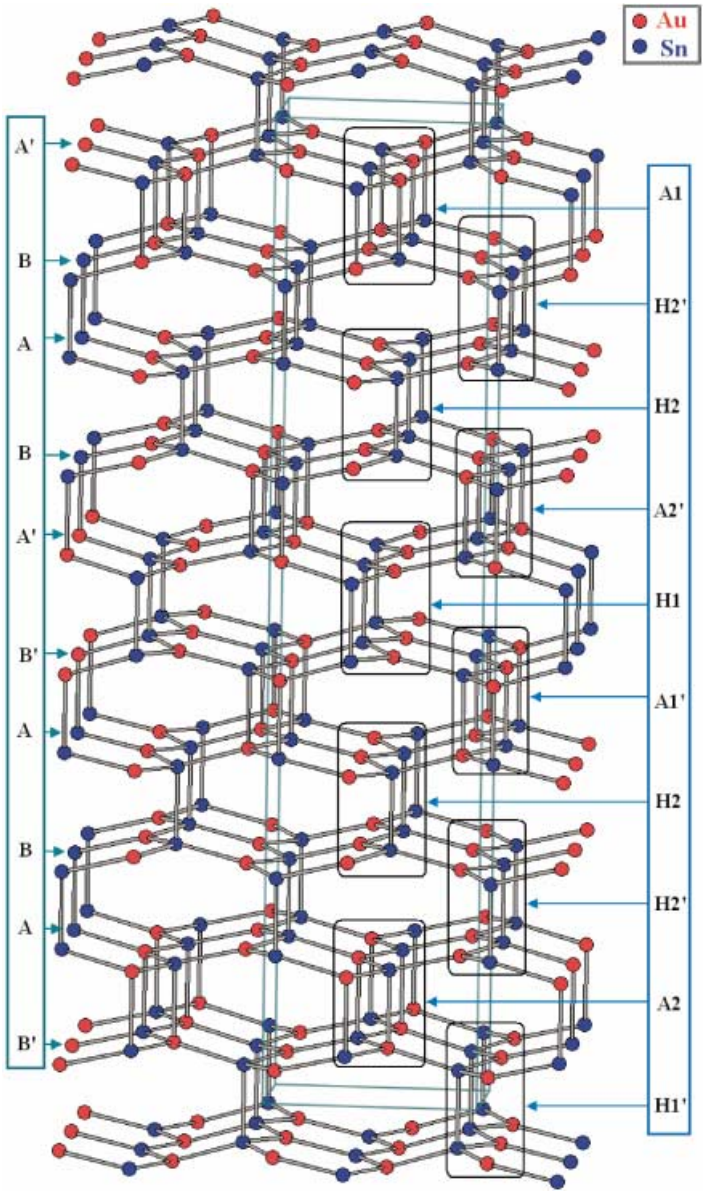

Fig. 2. *EuAuSn* (Au in red, Sn in blue) – *the thin green lines define the unit cell*. On the left side of the picture are designated all the layers present in the unit cell, and on the right (in the blue box) is given the succession of bonds (see text for details). Only the anionic $[AuSn]^{2-}$ sublattice is shown.

This is an indication that the simple *Zintl–Klemm* approach to bonding is not adequate. There must be other determinants of the structure and bonding, which we will eventually explore.

If one looks at *Fig. 2*, one sees that this elaborate structure is made up from layers. Not weakly bonded – on the contrary – but still layers. These are labeled **A**, **A′**, **B**, or **B′**. Each is a slightly puckered sheet of M : E (Au : Sn) stoichiometry. One such layer (**A′**) is shown from side and top views in *Fig. 3*.

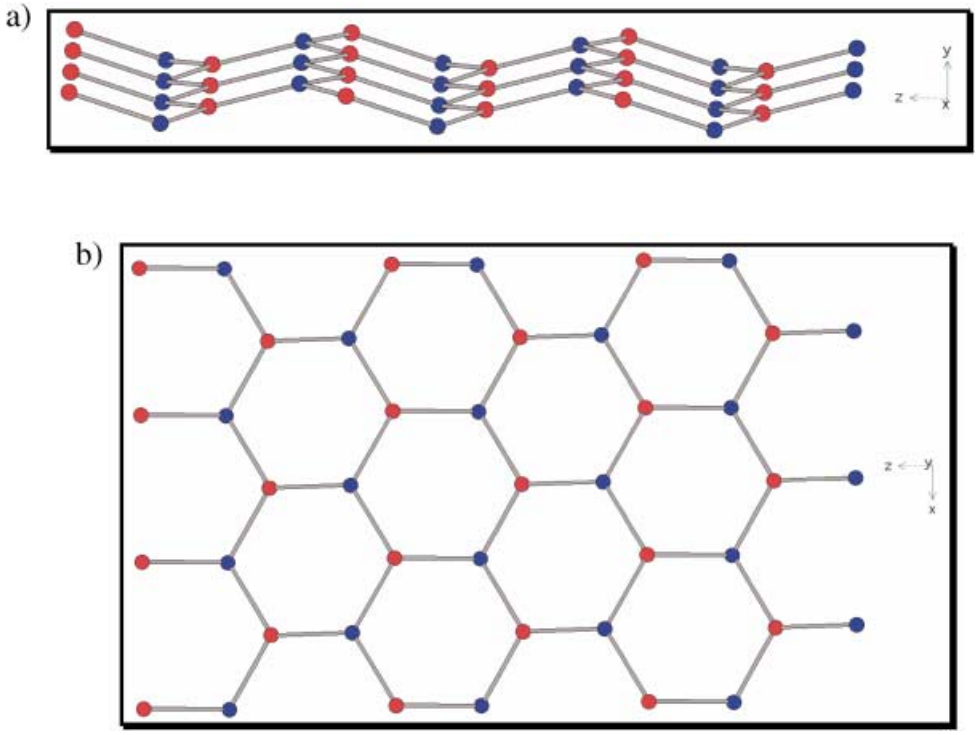

Fig. 3. *Side* (a) *and top* (b) *views of layer* **A′**

The slabs are ordered along the vertical direction in an 'eclipsed' way (so that the projection of all layers on an *xz*-plane, in *Fig. 2*, would simply look like the honeycomb sheet of *Fig. 3*,*b*, except for occasional Au/Sn interchanges in a sheet).

When the layers stack, they form either **A** (for **a**lternating) Au–Sn bonds, or **H** (for **h**omonuclear) Sn–Sn bonds. In the general case, there may also be M–M (that would be Au–Au here) **H**-type connections. The **A**, **A′**, **B**, **B′**, layering notation denotes distinct slabs, differing in puckering and Au/Sn position. In the next section, we will justify and make clear the distinction between them.

How does one decide whether a given atom is bonded to another? We decided (rather subjectively) to consider a Au–Sn, Sn–Sn, and Au–Au liaison relevant if it is within the interval 2.7–2.8 Å (region of strong covalent atom pair bonds) up to 3.15 Å (a separation found in many Au–Sn containing intermetallic compounds [4–12]). Beyond this limit, but shorter than a *Van der Waals* contact, structures often contain many weakly bonding interactions. These are interpretable as donor–acceptor associations. The o-REME structures contain these as well. Fully aware of the

arbitrariness of the procedure, we will not label these longer, weak interactions (of great interest to us, elsewhere) as bonds.

The individuality of the EuAuSn structure (and like ternaries containing M = Au, or M···M contacts, in general) is that there are no Au–Au bonds (as defined). The significant Au–Au separations in EuAuSn are in the interval 3.27–3.33 Å, exceeding the limits of typical bonds (2.88 Å in metallic Au) [13], being longer still than the weak, so-called 'aurophilic' interactions (mainly around 3.0–3.15 Å).

Returning to EuAuSn and focusing on the interlayer bonds present in the structure, one notices that there are no fewer than ten interlayer regions in the unit cell, of eight distinct types. These are labeled **A1**, **A2**, **H1**, **H2**, **A1′**, **A2′**, **H1′**, and **H2′** at the right of *Fig. 2*. As we mentioned above, **A** stands for **a**lternating (M–E) and **H** for **h**omonuclear (M–M and E–E) bonds. The 1, 2, prime, and unprimed suffixes distinguish bonds of each type, not equivalent by translational symmetry. The necessity for the notational system, which at this moment seems cumbersome, will be discussed in detail below.

The net result is that, perpendicular to the stacking direction in the $[AuSn]^{2-}$ sublattice of EuAuSn, there are four-, eight-, and ten-membered rings of alternating Au : Sn stoichiometry, as *Fig. 4* shows.

That concludes the geometric description of the anionic sublattice of EuAuSn. The reader might be discouraged by this (natural) complexity from thinking about the multitude of REME phases, so let's balance the picture with a simpler structure. An example is that of the isoelectronic compound EuAuGe, a clearly simpler REME. Its $[AuGe]^{2-}$ sublattice is shown in *Fig. 5*. The unit cell consists of just two layers, **A** and **B**, and has two kinds of interlayer bonds, **H2** and **H2′** (again, the 2, prime, and unprimed distinction will be addressed below).

The remaining REME structures lie in the rich territory in between these two poles. Let us next mention the variety of grounds for being interested in this class of compounds, and follow that with a rationale for the layer and bond-type distinction broached above.

What Is Interesting about REMEs? – Apart from the structural lure, much research in this area has been stirred by other practical and theoretical motivations. Here is a selection of them.

A) Nearly all the REME compounds have unusual *magnetic and electric properties*. The cation for most of these phases is a rare earth metal, sometimes magnetic, and in the anionic net there are transition metals, magnetic as well. There is much research concerned with the determination of these magnetic and electrical properties of REME phases [14–57], or even investigating the superconducting properties of certain phases [58–60]. Several reviews analyze these properties in depth, along with theoretical considerations on a number of such systems [61–65]. To be able to interpret how the characteristic magnetic moments work together, one must know the exact arrangement of the atoms in the structure. This is not always available from the experimental data; we will put forward a simple model for determining the potential layered networks as a function of the number of atoms per unit cell. Our eventual aim is to understand the reasons why some of these phases are insulators or semiconductors, and to learn the critical conditions for their metallization.

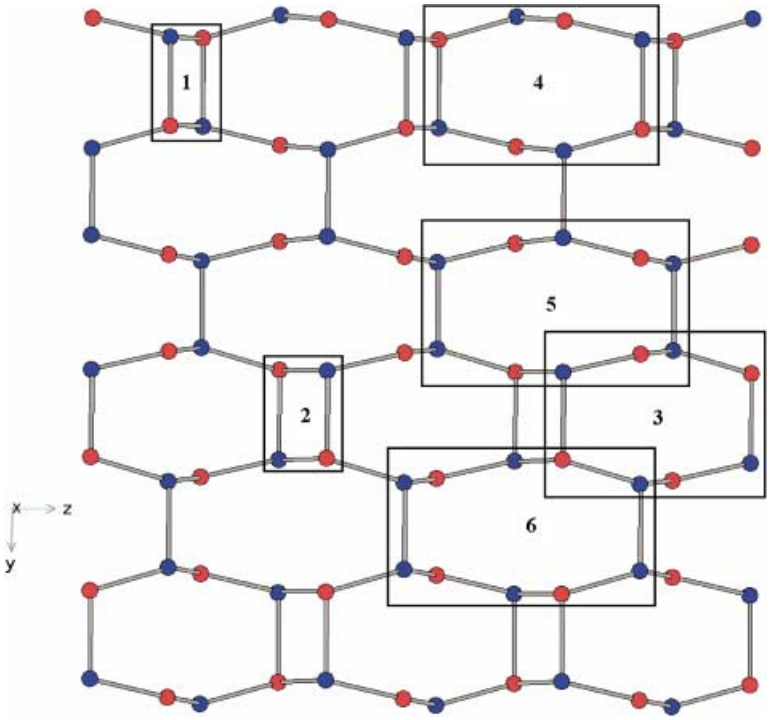

Fig. 4. *Projection perpendicular to the stacking direction of EuAuSn, showing four-, eight-, and ten-membered rings, emphasized by the numbered black rectangles. 1* and *2* enclose four-membered rings, *3* and *4* octagons, and *5* and *6* decagons.

B) Interesting *structural transitions* occur in these ternaries:

a) CaPtSi, for instance, changes from a 3- to a 4-connected net (see *Figs. 6*, *a* and *b*), under *pressure* [66][67].

b) Some REME systems display structural transformations where simultaneously the anionic network is internally reduced, accompanied by a change in the *oxidation state* of the countercations (when these are rare earths) [68][69]. This happens, for example, in the phase transition from α-Yb^{3+}PdSn to β-Yb^{2+}PdSn [70].

c) The *addition of hydrogen/deuterium* to some lattices produces a serious distortion. The anionic framework breaks down from an orthorhombic into a hexagonal type to accommodate the guest atoms. Instances of such alterations are known for LaNiSn [71], where the anionic $[NiSn]^{3-}$ sublattice collapses from a TiNiSi-type, orthorhombic unit, with 4-connected atoms and Ni–Sn bonds, into a hexagonal cell, with two-dimensional graphitic layers, composed of three-coordinate atoms, and Ni–Sn bonds. This resulting compound is $LaNiSnD_2$. A similar conversion takes place in the case of CeIrAl [72], which goes as well from an orthorhombic into a hexagonal unit cell upon hydrogenation, forming $CeIrAlH_2$. In CeIrGa [73], the insertion of H atoms takes place concomitantly with valence change (Ce goes from a mixed-valency to a $+3$ state). The end product is $CeIrGaH_x$, where $x \approx 1.7$. RENiIn (where RE = La, Ce, Nd) [74–76] undergo a similar transformation, to give $RENiIn_{4/3}$.

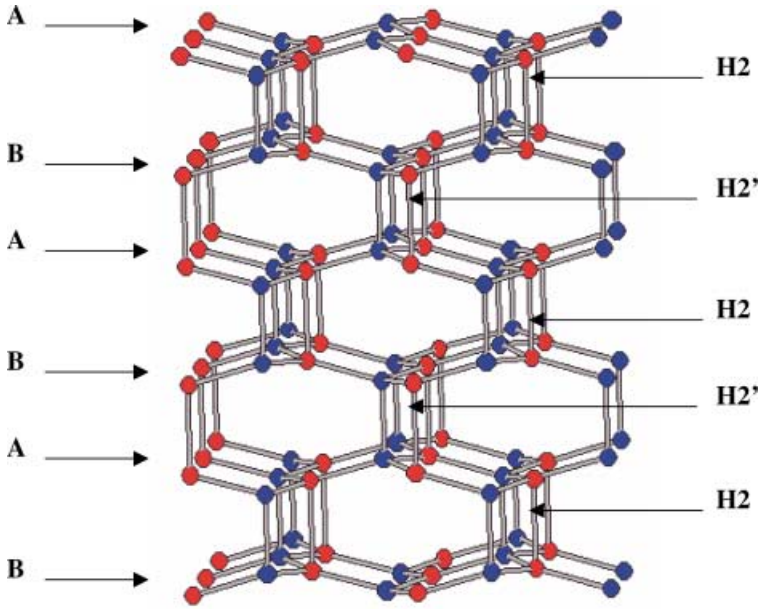

Fig. 5. *[AuGe]$^{2-}$ Sublattice of EuAuGe.* On the left side is given the layer sequence, and, on the right, the corresponding bond notation.

This process might be significant in two ways: *i*) REME materials could be potential candidates for hydrogen storage (in smaller, controllable quantities, though); *ii*) considering that hydrogen is not easily (or not at all) detectible by X-ray diffraction, one may well hope that, knowing the likelihood of a hydrogenation reaction, the structure could be correctly assessed. Thus, one could evaluate the contamination of a sample with H-atoms, just by examining the diffraction data and comparing them with an expected (or, eventually, theoretically predicted) structure.

C) A survey of the observed structures reveals (as we will describe in detail below) two kinds of *theoretically interesting series: a*) one for which the electron count varies widely, but the structure remains the same; *b*) a second one, where the lattice changes drastically, but the electron count is constant. The existence of such regularities poses a theoretical challenge.

It is essential at this point to define the way in which we count electrons; we will do so consistently throughout this series of papers. Considering that RE, in general, interacts with the residual network in a primarily ionic way, we assign its *n* valence electrons to the [ME] sublattice. For M, the transition metal, we add up all its outer (s and d) electrons, and, for E, we consider its valence shell, with s and p electrons. For example, in the EuAuSn case, because Eu donates two electrons to the anionic fragment, the total number of electrons for $[AuSn]^{2-}$ is: 2 (charge) + 11 (Au) + 4 (Sn) = 17 electrons. Another electron-counting scheme will be of subsequent interest – this treats the metal as a main group element, subtracting a filled d shell of ten electrons from the given electron count.

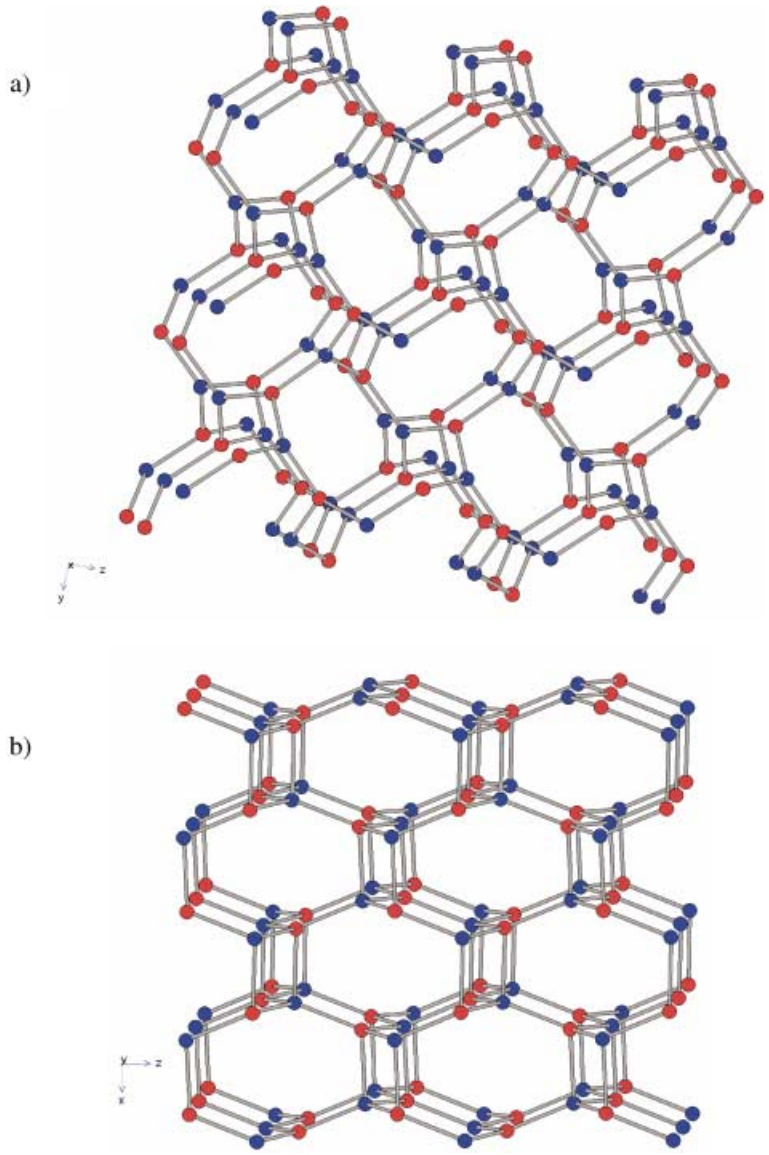

Fig. 6. a) *CaPtSi, low-pressure phase.* b) *CaPtSi, high-pressure modification*. Only the $[PtSi]^{2-}$ three-connected anionic network is shown. In red are Pt-atoms and in blue the Si-atoms.

Tracking the two series mentioned above is straightforward when one uses the *Appendix*. In *Table 2*, we give for each space group its representative structure type(s) and several examples of ternaries that have various electron counts. For example, the *Pnma* lattice is rather flexible electronically, accommodating from 15 to 18e^- per

$[ME]^{n-}$ anionic unit, as in CaPtGa ($15e^-$), SmRuGe ($15e^-$), CaPtGe ($16e^-$), YbAuGe ($17e^-$), ZrCuGe ($18e^-$), or TiNiSi ($18e^-$).

From *Table 3* (again in the *Appendix*), it is also apparent that, for a given electron count in the same REME subclass, there may be different structural realizations. Consider, for instance, the one where RE is a lanthanide (Ln), M belongs to group 11, and E is from group 3. For the *same electron count* of $17e^-/[ME]^{3-}$ unit, if Ln is taken in its usual $+3$ oxidation state, the 131 phases that we found crystallize in seven different lattices.

D) For many of these phases, it is difficult to obtain single crystals; only powder X-ray-diffraction data are available. Assignment of detailed atomic identities may be complicated when two elements have a similar number of electrons (*e.g.*, Ag and Sn). Theory could help here in shaping a model that would provide alternative yet chemically reasonable structures.

In the subsequent papers in this series, we will elaborate several construction principles for such a model based on the coloring problem.

Layers and Interlayer Bonds. – In the structures of EuAuGe and EuAuSn, we saw the extremes of simplicity and complexity in the REME networks. Let us now set down a way to look systematically at the variety of structures in between.

The common feature of the orthorhombic-REME (o-REME) structures (and not just of EuAuSn) are the layers of six-membered rings with 1:1 M to E stoichiometry, seen in *Fig. 3,b*, and *Fig. 7,b*, in a view along the stacking direction. Such two-dimensional layers are linked in the third (vertical, in *Figs. 2* and *4*) dimension, in an eclipsed manner, to build the o-REME structures. Inside one such (ME) layer there are only *alternating, or heteronuclear M–E bonds*; an explicit picture is shown in a top and side view in *Fig. 3,a*, and *Fig. 7,a*. The rings that form the 2D layers in EuAuSn are not planar (though there are numerous ternaries (not discussed here) that have planar 'graphitic' layers; these are present in h-REMEs). Within each hexagonal ring, three atoms go 'up' and three go 'down', relative to a median plane. This is most clearly seen, perhaps, in *Fig. 3,a*, and *Fig. 7,a*. The nonplanarity allows the generation, in principle, of three bonds with the layer above, and three with the layer below. Whether such bonds form and what type they are (EE, ME, MM) certainly varies in these compounds, and is a matter of critical concern to us. The type of unit cell that the crystal adopts, particularly the supercell, strongly depends on the interlayer bonds present in the network. In the specific case of the EuAuSn structure, interlayer Au–Sn and Sn–Sn associations form, but there are no Au–Au bonds (within the arbitrarily defined limit for an Au–Au 'bond' discussed above, of less than 3.15 Å). Although there are Au atoms sitting 'on top' of each other (and having the potential to form a bond), they tend to remain relatively far apart. Is there some electronic reason for that? We will approach this question in a sequel to this paper.

Let us introduce a notation for examining the stacking. The components of the notation are those translations that preserve 'eclipsing' and enable 'color changes' (interchanges of M and E). First, a layer **A** may be simply translated in the *xz*-plane, along the *z*-axis, by half of a unit cell, followed by a similar translation along the *x*-axis. This generates a distinct (as far as stacking is concerned) layer that we call **B** (see *Fig. 7* top). When *not* stacked, the isolated layers **A** and **B** are identical; in a stack they are

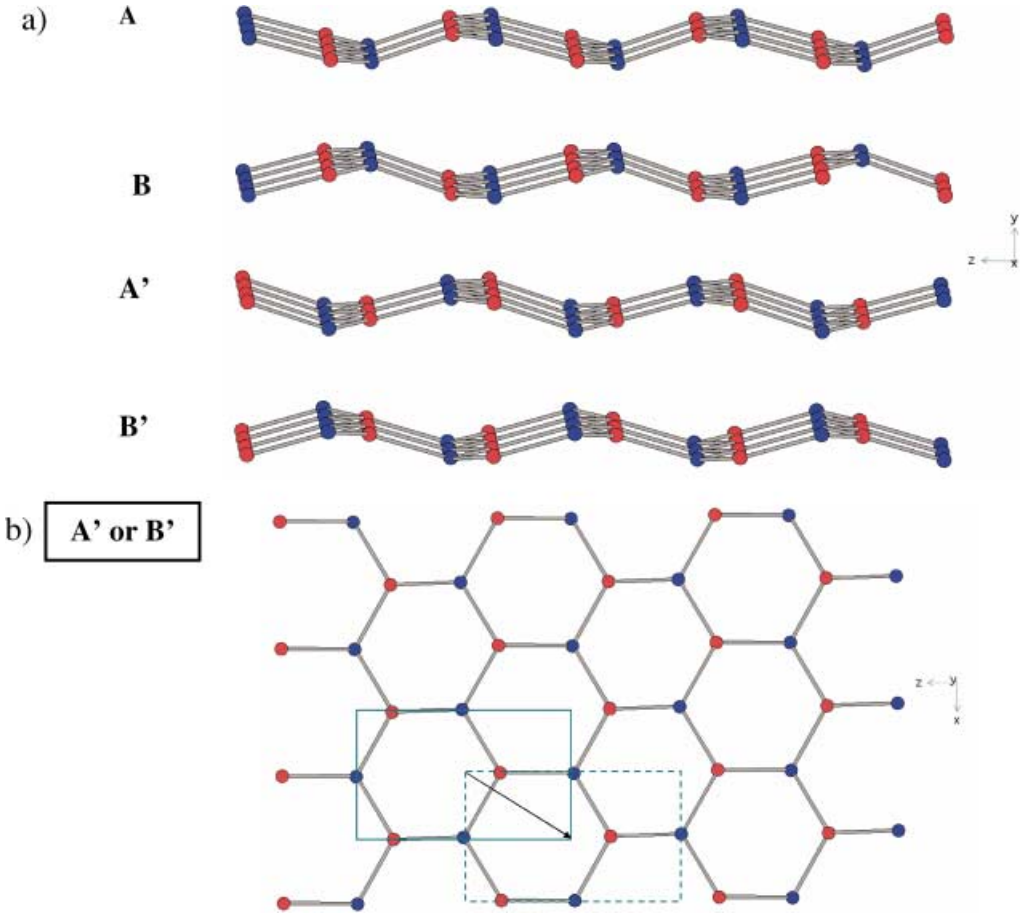

Fig. 7. a) *Side view of all layers found in EuAuSn*. Notice that **A** and **B** (**A′** and **B′**) have the same coloring, and the symmetry relationships between them are: a mirror plane and a translation by half of a unit cell along the *x*- and then *z*-axis. **A** and **A′** (**B** and **B′**) are parallel to each other, but have the colors of the atoms interchanged, whereas **A** and **B** (**A′** and **B′**) differ in their puckering in the *xz*-plane. b) *Top view* (along the *y*-axis) *of* **A′** *and* **B′** (linked to each other through a similar relationship as **A** and **B**), which, because of their same coloring in this projection, seem identical. The translation with $\frac{1}{2}\vec{x} + \frac{1}{2}\vec{z}$ of **A′** gives **B′**, easiest seen by following the 'movement' of the unit cell along the translating vector (black arrow) starting in the center of the rectangle outlined by solid green lines (unit cell for **A′**) to the center of the one having dashed lines (for **B′**).

distinct. If Au and Sn (atoms or positions) are just interchanged in **A**, then **A′** is created (we will call this a 'color change'). By translating **A′** within the *xz*-plane again, by $\frac{1}{2}\vec{x} + \frac{1}{2}\vec{z}$, one obtains the fourth (and last, if eclipsing is to be the rule) layer, **B′** (see *Fig. 7*). Layers **A** and **A′** are 'parallel' to each other (similarly for **B** and **B′**). **A** and **A′** are mirror images of **B**, and **B′**, respectively.

The four kinds of layers differ only in the presence of stacking. These slabs, by themselves, are related by simple symmetry operations that convert one into another layer, as *Fig. 7* illustrates.

The way these layers arrange along the stacking direction leads to different kinds of bonds between them (interlayer connections). Notice that only nonparallel layers can form such interlayer bonds generated by connecting those positions where a puckering 'up' of one layer is directly below a puckering 'down' of the layer above it. There are no such viable connections if the layers are parallel to each other, because there could be formed only four-membered rings along the stacking direction, which is not a consistent structural feature of o-REMEs.

To focus on the interlayer bond formation, we introduce a second notation that is sometimes convenient. We label with **H** the **h**omo-atomic (Au–Au or Sn–Sn, in EuAuSn) and with **A**, the hetero-atomic or **a**lternating (Au–Sn) bonds (see *Fig. 2*). Precisely as there are four layers, so there are four distinct (in the presence of stacking) **H**, and four distinct **A** bonds possible. For example, the succession of slabs **AB** generates **H1** bonds, from **BA** results **H1′**, and so on. All the correlations are shown below, in *Fig. 8*. *All* of them occur in EuAuSn and are labeled in *Fig. 2*.

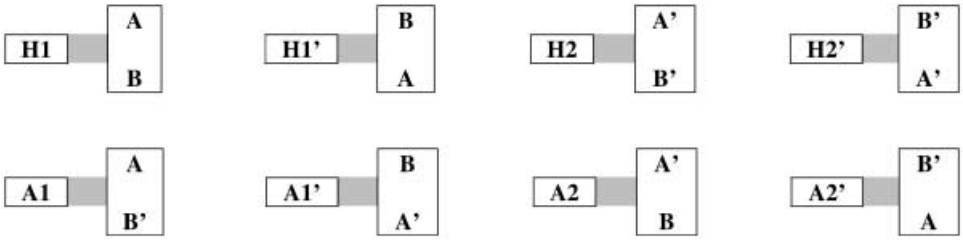

Fig. 8. *The relationship between bond types and layers*

Back to EuAuSn. – With these notations in place, we ask the reader to return to *Fig. 2*, to recognize the beautiful complexity of the EuAuSn structure. The full structure has an arrangement in which **A** (primed or unprimed) and **B** (primed or unprimed) slabs alternate, as they must, in a specific way: (**A′BABA′B′ABAB′**) . . . The variation in the ordering of different layers is impressive; EuAuSn is one of the most-elaborate representatives of this family that nature has granted us so far. It contains nearly every bonding situation that one could imagine within this context. We say this advisedly, having enumerated in a separate paper all the possible layer stacking sequences for unit cells containing up to ten layers per unit cell, and giving there some guidelines for selecting those likely to exist.

We now have the apparatus in place to survey systematically the many REME structures and pose the questions to which their structures and electron counts point.

Layering and Electron Counts in the REME Structures. – The complexity of the o-REME, h-REME and c-REME, t4-REME, t3-REME, and m-REME structures arises from all the possibilities of layering, the degree of distortion within one such slab, as well as the variability in interlayer bond formation. These structures are potential polytypes (with a relation to similar stacking arrangements found in the polytypes of MoS_2 and SiC), another manifestation of the richness of isomerism in three dimensions.

In *Table 2* (*Appendix*) and the *Supplementary Material*, we list and classify the known REME compounds by space group and structural type. We concentrate here on the layered anionic $[ME]^{n-}$ sublattices, discussing their connectivities. After illustrating the layered networks, we will introduce a selection of anionic networks *not* built up from slabs.

1. *Hexagonal Planar Slabs with No Strong Bonds* (just *Van der Waals* Interactions) *in the Stacking Direction, between Layers.* There are *ca.* 450 compounds of this type (records 3, 8, 9, 22, in *Table 2*). This is a rather numerous group; however, it is the one with the least diversity. It has unexceptionally one or two eclipsed graphitic layers per unit cell, hence three-connected M and E atoms, and solely M–E bonds. Two illustrative examples are ThAuSi ($19e^-$) and BaCdGe ($18e^-$), shown in *Fig. 9*. In ThAuSi [77] (like in CeNiSb ($18e^-$) [78]), there is only one layer per unit cell, with a layering of (**A**)**A**..., while BaCdGe [79] has two layers/unit cell, with every other slab changing 'color' along the stacking direction, and, therefore, generating the sequence (**AB**)**AB**... (where **B** is a layer with interchanged atomic positions relative to **A**). The electron count for this series is near $18e^-$/$[ME]^{n-}$ unit. The most frequently determined space groups are $P6_3/mmc$ and $P6/mmm$, but this structure is also found in $P\text{-}6m2$ and $P\text{-}3m1$.

A variation of this type occurs when M and E do not actually form bonds, but, instead, there are strong interactions between RE and E that give rise to hexagonal planar layers analogous to those we mentioned above for M and E. An example of this type is BaAuBi [80], where the main connections are within the [BaBi] plane (d_{Ba-Bi} = 2.82 Å, compare to 2.86 Å in the similar intermetallic BaAgBi [80]; in more-ionic compounds, this distance is much larger; in Ba_2Bi it is 3.722 Å, in Ba_5Bi_3 is 3.485, in $BaBi_3$ is 3.658 Å) [81–83]. Few such ternaries belong to the cubic space group, $F\text{-}43m$.

2A. *Networks in the EuAuSn Family.* As illustrated and discussed in detail for the complicated, but representative EuAuSn, the [ME] layers of the anionic network are somewhat distorted (see *Fig. 7*), with three atoms of the $(ME)_3$ hexagons going up and three down. Moreover, they are stacked in an eclipsed fashion. The number of slabs for each unit cell ranges from 2 to 10, with some variation in the layer sequence. These are, in principle, 4-connected nets.

The simplest of the frameworks of this type is the familiar two-layered TiNiSi structure [84][85], which is shown in *Fig. 10* (it was also shown in *Fig. 6*, *b*, earlier, as its variant, CaPtSi, but the layer notation was not stressed there). We clearly see the presence of four-, six-, and eight-membered rings. Note the 'ladders' generated by linking the four-membered ones perpendicular to the stacking direction, the **A**, **B′** layering, and the **A1** and **A2′** heteroatomic bonds.

The TiNiSi type is the most electronically flexible net. This family of compounds can accommodate from 15 to 18 electrons/$[ME]^{n-}$ unit (*e.g.*, RPtGa ($16e^-$) [86], RPtIn ($16e^-$) [87], CaAuE ($16e^-$), E = Al, Ga, YbMAl, M = Pd ($16e^-$), Pt ($16e^-$), Au ($17e^-$) [39]). In a previous study, *Landrum* and co-workers [88][89] analyzed the bonding within this structural type, in the series of compounds MTSi, where M is a 3d metal, and T is Co, Ni, and Cu. They were interested in a similar problem, namely: what happens to a lattice upon adding electrons to it. Up to what point does its structure remain unchanged? The conclusion reached in their work was that, because nonbonding states of [TSi] are being filled upon adding a countercation, M, richer in electrons, there is

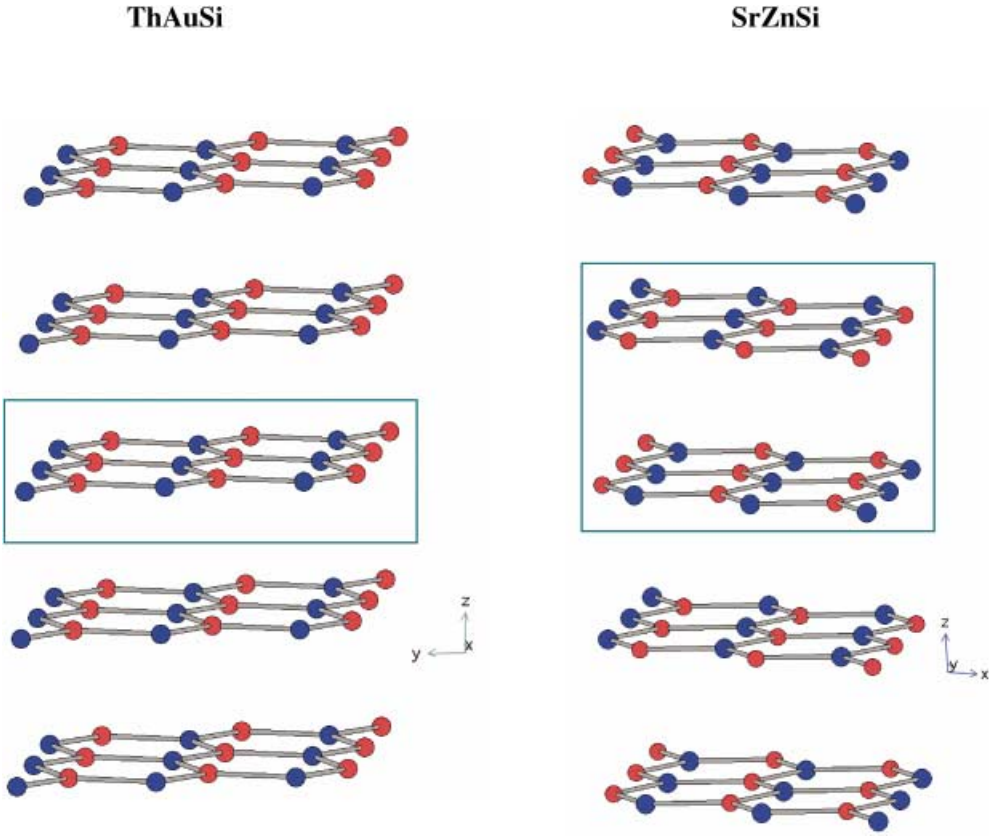

Fig. 9. *Within the green lines is the repeating layer sequence in ThAuSi* (left) *and SrZnSi* (right)

little or no major alteration of the geometry. However, there is one point at which M–M bonding levels begin to fill, and this seems to be for M = Fe. This structure distorts significantly, a fact rationalized as a consequence of Fe–Fe bond formation.

Space groups: *Pnma*, *Imma*, *Pna*2_1, *Pmmn*. There are *ca.* 650 compounds in this group, thus being the best represented in the whole REME family. Variations on this theme exist, incorporating an (**AB**)**AB**... progression (*e.g.*, EuAgGe [90]), more-complicated four layered cells (**ABA′B′**)**ABA′B**... (SmPtGe [91]), or even more-elaborate sequences, as the unit cell increases. The number of layers/unit cell may be 2, 4, 6, or 10. Certain ternaries contain all four types of two-dimensional layers stacked in very different ways, generating along this axis different homonuclear, **H** (M–M or E–E), and alternating, **A** (M–E), bonds along the stacking directions. The most-common electron count is *ca.* 17e$^-$/[ME]$^{n-}$ unit, although, as we noted, it may vary (*Entries 1*, *5*, *16*, and *17* in *Table 2*).

2B. *Uncolored Lattices.* Although not a distinct group by its layers or stacking, this category includes all the crystallographically 'unresolved' structures, the ultimate structural challenge in the whole o-REME class.

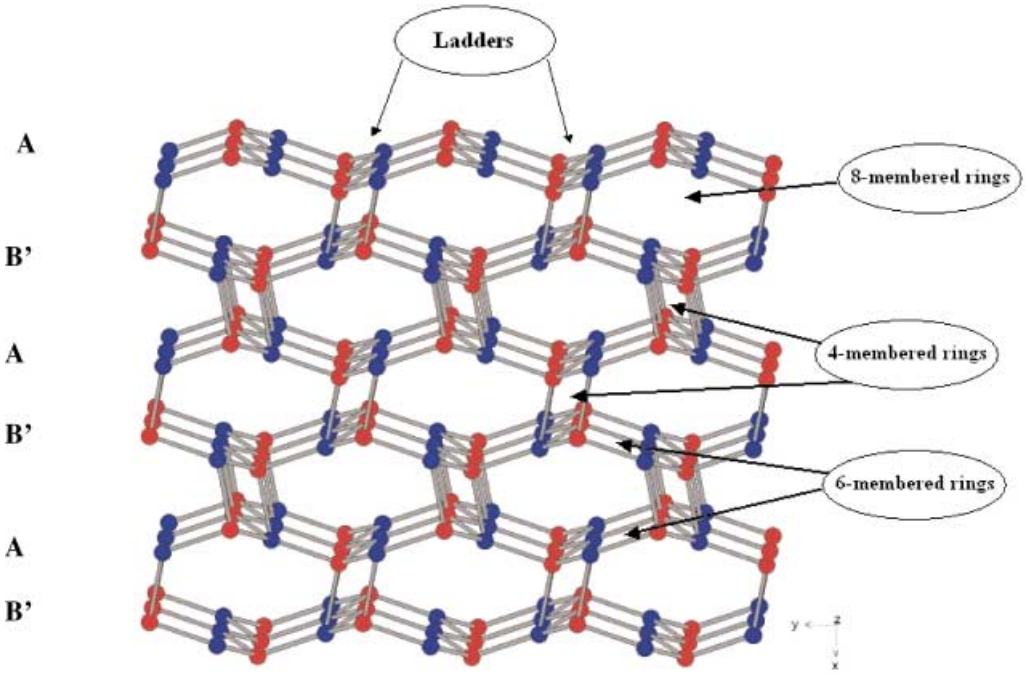

Fig. 10. *TiNiSi – only the [NiSi] four-connected anionic network is shown*. In red is Ni, and in blue is Si. The repeating layering sequence is (**AB′)AB′**... Note the four-, six-, and eight-membered rings, and the ladders generated by the four-membered rings.

These uncolored lattices, with puckered layers approximating in their degree of distortion those of EuAuSn, are derived from the $CeCu_2$ (essentially the same structural type as TiNiSi) or KHg_2 families [92][93] (see *Fig. 11*), and likewise, 4-connected nets. Two indicative examples are EuAgSn [94–96] and EuZnGa [97]. Crystallographic studies of these point either to a statistical distribution of the atoms in the structure or to that one cannot distinguish between M and E when they have similar electronic densities. The most-common electron count in this last class is around $17e^-/[ME]^{n-}$ unit, and they are formulated usually in the Imma setting (*Entry 5* in *Table 2*).

3. *Planar and Puckered Layers inside of the Same Unit Cell, Forming 3- and 4-Connected Nets by Interlayer Bonding*. Within the unit cell, there are usually two types of eclipsed layers: one is planar, graphitic, with three-coordinated M and E atoms, exclusively M–E bonded within the layer. These are isolated by the rest of the anionic assembly. Next to it, follow two other slabs, more distorted, with distinct chair hexagons, remnants of a wurtzite-type lattice. These latter ones have M–E interlayer bonds, but E–E interlayer connections; M being three- and E four-coordinated. YbAgSn [98–103], one example from this family, is shown in *Fig. 12*. Another possible arrangement is planar–puckered–planar. The most-common electron count is *ca.* 17–$18e^-/[ME]^{n-}$ unit and the space groups are *P*–6*m*2 and *P*3. We have found 12 compounds in this series (*Entry 9* in *Table 2*).

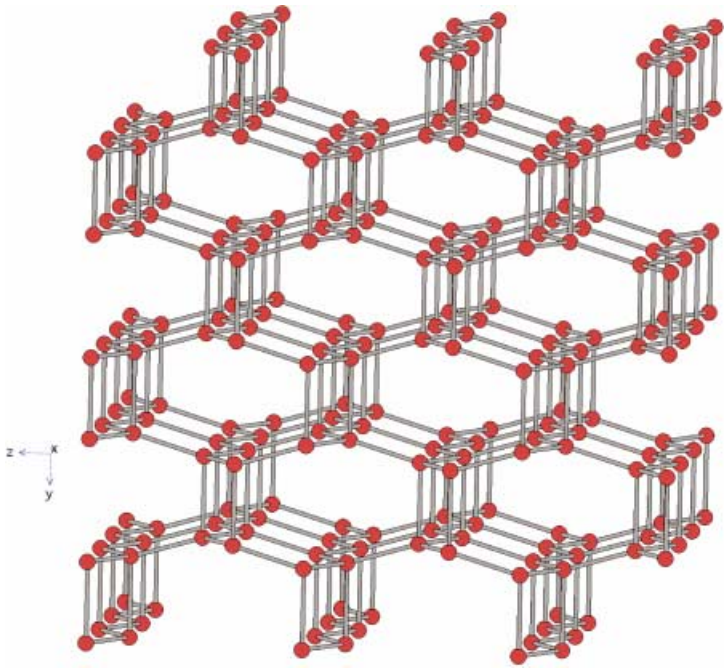

Fig. 11. *$CeCu_2$ framework*. For clarity, only the four-connected Cu (red) sublattice is given.

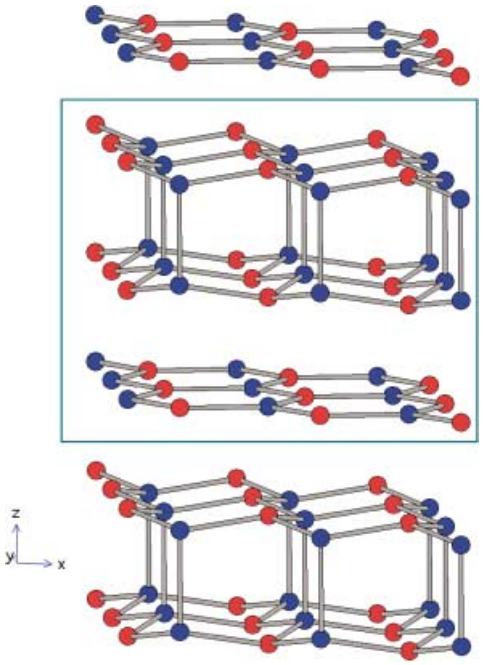

Fig. 12. *The unit cell with puckered-puckered-planar layers of YbAgSn is shown in green*

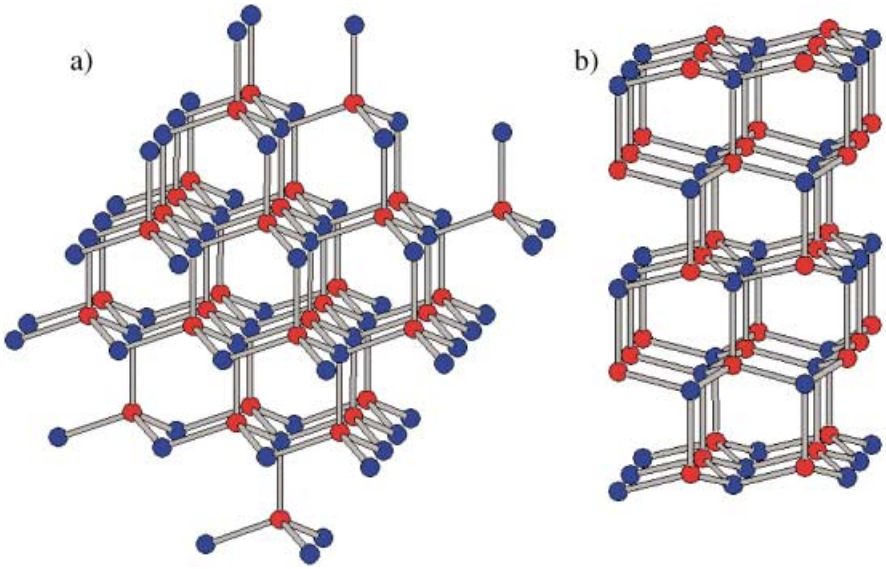

Fig. 13. a) *Sphalerite-type anionic net of MgAuSn*. b) *Wurtzite-type anionic lattice of LuAuGe.*

4. *Strongly Puckered Layers with a 4-Connected, Diamond-Like Structure*. These compounds are composed of layers as distinctly distorted as in the diamond lattices and, thus, acquire structures of either sphalerite or wurtzite type, depending on their stacking. Both of these categories have only M–E bonds. HoAuSn, MgAuSn, or ThNiSn are several examples of the first type (and, thus, have the layers staggered in the stacking direction), and GdAuSn, DyCuSn, or LuAuGe of the latter – with slabs eclipsed (*Fig. 13*). The most-common electron count is *ca.* 18–19e$^-$/[ME]$^{n-}$ unit. In the space groups *F*-43*m*, *Fd*-3*m* (blende, *Entries 4* and *15* in *Table 2*), we found *ca.* 180 compounds, and in $P6_3mc$ (wurtzite) *ca.* 50 phases (*Entries 7* and *8* in *Table 2*).

In an analogous wurtzite environment, there is a slightly different bonding polytype, having within layers M–E bonds, but as interconnecting liaisons M–M and E–E (*e.g.*, LuAuSi). We found *ca.* 10 examples of such less-familiar compounds, crystallizing in *P*-6*m*2 groups (*Entry 9* in *Table 2*).

REME Ternaries also form different structures without distinct layers. We will mention them briefly. These structures might prove useful for comprehending the mechanisms of structural transformation under the influence of external factors.

5. *Structures with 3-, 4- and 6-Connected Atoms*. An example is YbAgGe (17e$^-$) [104], shown in *Fig. 14*. These are complex networks (there are *ca.* 500 examples, listed in *Table 2*, *Entries 2*, *14*, and *21*) that can hold between 15 and 19e$^-$/[ME]$^{n-}$ unit (*e.g.*, PrRhIn [0]–15 e$^-$), 18e$^-$ being the most frequently encountered. Common space groups are: *P*-62*m*, *Im*2, and *P*-6*mc*. In these structures, M is tetrahedrally coordinated, whereas E is either trigonal planar, or octahedral. Generally, only M–E contacts are present.

6. *Three Connected Nets that Contain Helical Chains in One Direction, Running Half Clockwise and Half in the Other Direction, or All Having the Same Twist*. In this

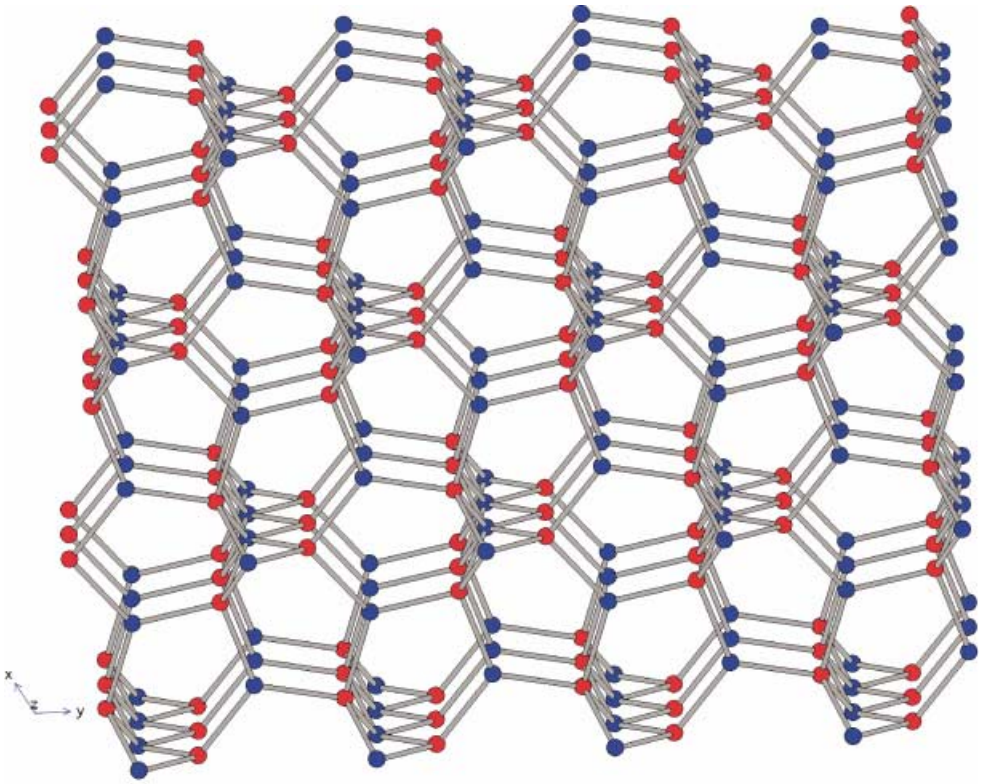

Fig. 14. *YbAgGe – only [AgGe] three-, four-, and six-connected anionic network is illustrated*. In red is Ag and in blue is Ge.

case, too, the networks are formed entirely from M–E bonds, and M and E are three-connected. See *Fig. 6,a*, where the structure of one low-pressure variant of CaPtSi is shown. The electron count usually is $16e^-/[ME]^{n-}$ unit. Their common space group is $P2_13$. We found 30 examples (*Entry 10* in *Table 2*).

This completes the rough survey of the structural richness in the REME series. In the next paper, we will take the significant and diverse subset containing the layered structures, of which EuAuSn is a member, and ask whether all geometrically possible networks have been realized, and whether there is some regularity governing their appearance.

We are grateful to the *National Science Foundation* for its support of this research under grant No. NSF DMR 0073587.

Appendix. – Within the CRYSTMET and ICSD databases, we found more than 2000 REME species crystallizing in a limited number of unit cell types. We see *ca.* 35 types of unit cells, of which about nine or ten contain the greatest part of them all. In *Table 2* are listed all the space groups we came across (ranked simply by frequency of occurrence: the synthesizers' popularity poll). We annotate this table by remarks on their distinctive structural characteristics. In *Table 3* are given detailed data on the individual unit cells in each REME subclass.

Table 2. *Space Groups, Representative Structure Types, and Number of Compounds within RE M E Family, along with Common Electron Counts per [ME] Anionic Unit* (the underlined number is the one most often encountered). See body of paper for definition of electron count. We also list some examples, with their electron counts per ME unit, in parentheses, and mention some typical features of the anionic networks, $[ME]^{n-}$. In the last column, '*Analogous*' , the numbers refer to other structurally similar space groups (an illustration of a representative structure for each space group listed below is given in the *Supplementary Material* for this paper).

Rank	Space group (#)	Structure type	No. of phases	No. e^-/[ME]	Examples (No. e^-/[ME])	Comments	Analogous
1	*Pnma* (62)	Co_2Si, TiNiSi, CaPdAs, BaNiN, YbAuGe, CaCuGe, CaAuSn	540	15 – 18	CaPtGa(15), SmRuGe(15), CaPtGe(16), YbAuGe(17), ZrCuGe(18), TiNiSi(18)	*Orthorhombic*-REME (O-REME) TiNiSi – type 2L/unit cell, or *n*L/unit cell 4-connected networks M–E bonds within one layer, and M–E or (M–E, M–M and E–E) bonds between layers	5, 16, 17
2	*P*-62*m* (189)	Fe_2P	477	15 – 18 – 19	ScRuGe(15), HfFeGe(16), ThCoSn(17), GdAgGe(18), CaAgAs(18), KZnAs(18), YbCdSn(18), ThAuSi(19)	*Hexagonal*-REME (H-REME) 3, 4, 6 connected networks (M is 4, and E is 3- and 6-connected) M–E bonds	13, 21
3	$P6_3/mmc$ (194)	$CaIn_2$, $MgZn_2$, Ni_2In	396	15 – 18	GdCoAl(15), BaAgAs(18), CaCuAs(18), DyCuSi(18), SmPtAs(18)	H-REME Graphitic layers, with 2L/unit cell 3-connected networks M–E bonds	8, 9, 22
4	*F*-43*m* (216)	LiAlSi, MgAgAs	171	13 – 18	LiRhIn(13), LiAuAl(15), MgAuSn(17), MgNiSb(17), ScPtSn(17), LiZnN(P)(18), ScAuSn(18), YPtSb(18), ThNiSn(18)	*Cubic*-REME (C-REME) Blende lattice 4-connected networks M–E bonds	15
5	*Imma* (74)	$CeCu_2$	99	17 – 18	CaAgGe(17), YbAuGe(17), GdPdSi(17), SmPtGe(18), UPtSi(18)	O-REME $CeCu_2$-2L/unit cell 4-connected networks M/E atomic positions not determined	1, 16, 17
6	*P*4/*nmm* (129)	Cu_2Sb	83	14 – 18	LiFeAs(P)(14), CeOs(Ru)Si(15), NdFeSi(15), TbCoSi(16), MgCuAs(18), NaZnAs(Sb)(18)	*Tetragonal*-REME (t4-REME) $BaAl_4$ or $ThCr_2Si_2$ – type 4, 8-connected networks (M is 8- and E is 4-coordinated) M–M and M–E bonds	

Table 2 (cont.)

Rank	Space group (#)	Structure type	No. of phases	No. e^-/[ME]	Examples (No. e^-/[ME])	Comments	Analogous
7	$P6_3mc$ (186)	LiGaGe	50	18–19	YAuSi(Ge)(18), SmPdAs(18), YbAuSb(18), TbCuGe(18), ScAuGe(18), LiZnBi(18), UCuGa(18), EuCdPb(18), UAuSn(19)	H-REME Wurtzite 4-connected networks M–E bonds	9
8	$P6/mmm$ (191)	AlB_2	45	18	NdNiSb(18), PrCuGe(18), YCuSi(Ge)(18), NdCuSi(Ge)(18)	H-REME Graphitic layers, with 1L/unit cell; atomic positions are not determined. 3-connected networks M–E bonds	3, 9, 22
9	$P\text{-}6m2$ (187)		39	17–18	LuPtP(18) LiZnGe(17) REAuSi (RE = U, Th, Sc, Lu)(18–19) LiNiN(16), BaPtSb(17), LuPtP(18), KZnSb(As)(18)	H-REME	
		AlB_2				1. Graphitic layers 1L/unit cell 3-connected networks M–E bonds	3, 8, 22
		LiGeZn				2. Two diamond layers, in a wurtzite arrangement, forming a 4-connected fragment, with M–E intralayer bonds, and E–E between slabs, and one additional isolated graphitic layer (3-connected sheet, with M–E bonds)/unit cell.	3, 7, 8, 9
		ScAuSi				3. Wurtzite structure 4-connected networks M–E bonds within layers, and M–M and E–E interlayer bonds	7
10	$P2_13$ (198)	NiSbS, $SrSi_2$	30	16	LaIrSi(15), BaIrP(16), CaPtSi(16), EuPtGe(16), BaPtAs(P)(17)	C-REME Helical 1-D chains intertwined in a 3-D array 3-connected networks M–E bonds	

Table 2 (cont.)

Rank	Space group (#)	Structure type	No. of phases	No. e^-/[ME]	Examples (No. e^-/[ME])	Comments	Analogous
11	$I4_1md$ (109)	CaPtAs	22	17	Ca(Eu)PtAs(17), LaPtSi(17), LaNiSi(17)	T4-REME *trans*-Polyacetylene chains running in two perpendicular directions, linked in a 3-D framework (with 4 or 12 such ME, polyacetylenic, zigzag chains/unit cell) 3-connected networks M–E bonds	18
12	$P4_2/mmc$ (131)	YCoC	18	17	YCoC(16), CaNiN(17)	T4-REME Linear, 1-D, chains running in two perpendicular directions 2-connected networks M–E bonds	14
13	*Ima*2 (46)	TiFeSi	16	16	ZrRuGe(16), TiFeSi(16)	O-REME 3-, 4-, 6-connected (M is 4, and E is 3- and 6-connected) M–E bonds	2, 21
14	*P*4/*mmm* (123)	YCoC	13	16	TmCoC(16)	T4-REME 2-D sheets with 2 (E)- and 4 (M)-connected atoms M–E bonds	12
15	*Fd*-3*m* (227)	$MgCu_2$	8			C-REME Blende lattice 4-connected networks M/E positions not determined	4
16	$Pna2_1$ (33)	NaAuSn	8	16–17	NaAuSn(16), CaCuGe(17)	O-REME TiNiSi type, with **2L**, **6L**/unit cell 4-connected networks M–E bonds within one layer, and M–E or (M–E, M–M and E–E) bonds between layers	1, 5, 17
17	*Pmmn* (59)	GdPdGe	5	17	(Gd)ErPdSi(17), (Sm)CePtGe(17), GdPdGe(17)	O-REME TiNiSi type, with **4L** 4-connected networks M–E bonds within one layer, and M–E, M–M and E–E bonds between layers	1, 5, 16
18	$I4_1/amd$ (141)	$ThSi_2$	5			T4-REME *trans*-Polyacetylene chains running in two perpendicular directions, linked in a 3-D framework (with 4 polyacetylenic M–E chains/unit cell) 3-connected networks M/E positions not determined	11
19	*Fm*-3*m* (225)	CaF_2	4			C-REME Face-centered cubic	

Table 2 (cont.)

Rank	Space group (#)	Structure type	No. of phases	No. e^-/[ME]	Examples (No. e^-/[ME])	Comments	Analogous
20	*Pm*3*n* (223)		4			C-REME M–M, and M–E bonds	
21	*P*-62*c* (190)		4			H-REME 3-, 4-, 6-connected networks (M is 4, and E is 3- and 6-connected) M–E bonds	2, 13
22	*P*-3*m*1 (164)	$CeCd_2$	4	17	EuPtP(17)	Trigonal-REME (t3-REME) Graphitic layers, with 2L/unit cell 3-connected networks M–E bonds	3, 8, 9
23	*C*2/*m* (12)	SrAgGe	4	14–17	YbFeGe(14), SrAgGe(17), CaAuGe(17)	Monoclinic-REME (m-REME) 3- and 4-connected networks M/E positions not determined	
24	*I*4/*mmm* (139)		2			T4-REME	
25	$Pmc2_1$ (26)	CaPtP	2			O-REME	
26	$P2_1/c(n)$ (14)	$CoSb_2$	2			M-REME	
27	*Fddd* (70)	LiIrB	1			O-REME	
28	*Im*3 (204)	LiCuSi	1	16	LiCuSi(16)	C-REME	
29	*P*3 (143)	LiZnGe	1			T3-REME	
30	*Pbcm* (57)		1			O-REME	
31	C2/c (15)	BaCuN	1			M-REME	
32	$P112_1/m$ (11)		1			M-REME	
33	*P*42/*mnm* (136)	TiPtSi	1		TiPtSi(18)	T4-REME	
34	*Cmc*21 (36)	AgCuS	1			O-REME	
35	*Cmca* (64)	BaPdP	1		BaPdP(17)	O-REME	
36	?		2				
Total			2063				

Table 3. *Classification of REME Phases, as a Function of the Number of Compounds Crystallizing in the Same Space Group* (in the *Supplementary Material* of this paper, we list the compounds, and their corresponding space groups, with their bibliographic data, as well as show some representative structures)

REME	Space group	No. of compounds
(1)(8–10)(13)	*F*-43*m*	9
	Fddd	1
(1)(8–10)(14)		0
(1)(8–10)(15)	*P*4/*nmm*	3
(1)(11)(13)	*F*-43*m*	1
(1)(11)(14)	$Pna2_1$	1
	*Im*3	1
(1)(11)(15)	*P*3	1
(1)(12)(13)		0
(1)(12)(14)	*P*-6*m*2	1
(1)(12)(15)	*P*4/*nmm*	6
	F-43*m*	5
	$P6_3/mmc$	4
	$Pna2_1$	2
	Pnma	2
	P-6*m*2	2
	$P6_3mc$	2
(2)(8–10)(13)	*Pnma*	5
	Pbcm	1
(2)(8–10)(14)	$P2_13$	11
	Pnma	7
	?	2
	$P2_1/c(n)$	2
	P-62*m*	1
(2)(8–10)(15)	*Pnma*	9
	$P2_13$	5
	P-6*m*2	4
	$P4_2/mmc$	3
	F-43*m*	3
	$Pmc2_1$	2
	$I4_1md$	2
	$P6_3mmc$	2
	Cmca	1
(2)(11)(13)	$P6_3/mmc$	4
	Pnma	3
	Imma	1
(2)(11)(14)	*Pnma*	4
	F-43*m*	3
	*C*2/*m*	1
	$Pna2_1$	1
(2)(11)(15)	$P6_3/mmc$	30
	F-43*m*	4
	P-62*m*	3
	$P6_3mc$	2
	Pnma	2
	*C*2/*c*	1
	*P*4/*nmm*	1

Table 3 (cont.)

REME	Space group	No. of compounds
(2)(12)(13)		0
(2)(12)(14)	$P6_3/mmc$	1
(2)(12)(15)		0
(3)(8–10)(13)	*Pnma*	16
	P-62*m*	12
	$P6_3/mmc$	8
	$P112_1/m$	1
	Imma	1
(3)(8–10)(14)	*Pnma*	47
	P-62*m*	20
	*P*4/*nmm*	11
	*I*41*md*	6
	Imma	4
	$P2_13$	3
	*P*4/*mmm*	1
	$P4_2/mmc$	1
	F-43*m*	1
	*Pm*3*n*	1
	*Fm*3*m*	1
(3)(8–10)(15)	*F*-43*m*	12
	$P6_3/mmc$	8
	P-62*m*	3
	Pnma	2
	*P*4/*nmm*	1
(3)(11)(13)	*P*-62*m*	8
	Imma	3
	Pnma	2
	$P6_3/mmc$	1
(3)(11)(14)	*P*-62*m*	14
	$P6_3/mmc$	12
	$P6_3mc$	4
	F-43*m*	3
	*P*6/*mmm*	3
	Pnma	2
(3)(11)(15)		0
(3)(12)(13)	$P6_3/mmc$	7
	Imma	1
(3)(12)(14)	*P*6/*mmm*	1
(3)(12)(15)		0
(4)(8–10)(13)	$P6_3/mmc$	15
	P-62*m*	13
	P-62*c*	1
	F-43*m*	1
(4)(8–10)(14)	*Pnma*	36
	F-43*m*	19
	P-62*m*	18
	*Ima*2	16
	P-62*c*	2
	$P6_3/mmc$	2
	$P4_2/mnm$	1

Table 3 (cont.)

REME	Space group	No. of compounds
(4)(8–10)(15)	*Pnma*	23
	P-62*m*	22
	F-43*m*	15
	Imma	3
	Pnam	2
	$P6_3/mmc$	2
(4)(11)(13)	$P6_3/mmc$	9
	P-62*c*	1
(4)(11)(14)	*Pnma*	13
(4)(11)(15)		0
(4)(12)(13)	*Fd*-3*m*	1
(4)(12)(14)		0
(4)(12)(15)		0
(Ln)(8–10)(13)[a])	*P*-62*m*	114
	Pnma	96
	$P6_3/mmc$	56
	*C*2/*m*	3
	Pnam	2
	Imma	1
	P-3*m*1	1
(Ln)(8–10)(14)	*Pnma*	202
	P-62*m*	60
	*P*4/*nmm*	54
	Imma	37
	Pnam	19
	$P4_2/mmc$	14
	*P*4/*mmm*	12
	$I4_1md$	11
	$P2_13$	10
	Pmmn	5
	$Pna2_1$	3
	?	3
	*P*6/*mmm*	2
	*Pm*3*n*	2
	*Fm*3*n*	1
	*I*4/*mmm*	1
(Ln)(8–10)(15)	*F*-43*m*	61
	$P6_3/mmc$	54
	Pnma	9
	P-62*m*	8
	*P*4/*nmm*	7
	*P*6/*mmm*	7
	$P6_3mc$	5
	$I4_1md$	3
	P-6*m*2	2
	?	2
	Imma	1
	$P2_13$	1
	P-3*m*1	1

Table 3 (cont.)

REME	Space group	No. of compounds
(Ln)(11)(13)	*P*-62*m*	74
	Imma	34
	Pnma	16
	$P6_3/mmc$	7
	Fd-3*m*	7
	*P*6/*mmm*	2
	Fm-3*m*	1
(Ln)(11)(14)	$P6_3/mmc$	87
	P-62*m*	25
	$P6_3mc$	17
	*P*6/*mmm*	17
	F-43*m*	9
	?	3
	Imma	3
	Pnma	2
	*I*4/*mmm*	1
	P-6*m*2	1
	$Pna2_1$	1
(Ln)(11)(15)	$P6_3/mmc$	13
	$P6_3mc$	6
	F-43*m*	1
	Pnma	1
(Ln)(12)(13)	$P6_3/mmc$	39
	P-62*m*	6
	Imma	4
	*P*6/*mmm*	1
(Ln)(12)(14)	*P*6/*mmm*	12
	$P6_3mc$	7
	$P6_3/mmc$	4
	P-62*m*	3
	Imma	3
	Pnma	2
(Ln)(12)(15)		0
(An)(8–10)(13)[b])	*P*-62*m*	55
	$P6_3/mmc$	20
	Pnma	3
	Imma	2
(An)(8–10)(14)	*P*-62*m*	19
	F-43*m*	18
	Pnma	9
	Imma	5
	$P6_3mc$	5
	$I4_1/amd$	5
	Pnam	3
	$P6_3/mmc$	2
	*Pm*3*n*	1
	$Cmc2_1$	1
(An)(8–10)(15)	*F*-43*m*	6
	$P6_3/mmc$	2
	P-62*m*	1

Table 3 (cont.)

REME	Space group	No. of compounds
(An)(11)(13)	*Imma*	4
	$P6_3/mmc$	3
	Pnam	1
	$P6_3mc$	1
(An)(11)(14)	*P*-6*m*2	4
	$P6_3/mmc$	4
	P-3*m*1	2
	Imma	2
	$P6_3mc$	1
(An)(11)(14)		0
(An)(11)(15)		0
(An)(12)(13)		0
(An)(12)(14)		0
(An)(12)(15)		0

[a]) Ln: Lanthanide element. [b]) An: Actinide element.

Supplementary Material. – In this section (available on request) we include the following: *1*) A list with all REME compounds found in CRYSTMET and ICSD, their structure type (if available), space group, and *Z* (number of formula units) in unit cell. Subsequently, we provide a table with references for each compound specified above. *2*) We provide 28 pictures of the most-representative REME compounds, one from each grouping in *Table 2* (*Appendix*). These illustrate visually the comments given in *Table 2* concerning the structural characteristics present in each grouping.

REFERENCES

[1] The Metals Database, Version 1.10 of the CRYSTMET Search program, Toth Information Systems, Inc.
[2] Inorganic Crystal Structure Database (ICSD), FIZ Karlsruhe, Germany and The National Institute of Standards and Technology, USA.
[3] R. Pöttgen, R.-D. Hoffmann, R. Mullmann, B. D. Mosel, G. Kotzyba, *Chem.–Eur. J.* **1997**, *3,* 1852.
[4] J. S. Charlton, M. Cordey-Hayes, I. R. Harris, *J. Less-Common Met.* **1970**, *20*, 105.
[5] J.-P. Jan, W. B. Pearson, A. Kjekshus, S. B. Woods, *Can. J. Phys.* **1963**, *41*, 2252.
[6] S. Stenbeck, A. Westgren, *Z. Phys. Chem. B* **1931**, *14*, 91.
[7] G. Wrobel, H. U. Schuster, *Z. Anorg. Allg. Chem.* **1977**, *432*, 95.
[8] U. Eberz, W. Seelentag, H. U. Schuster, *Z. Naturforsch. B: Anorg. Chem. Org. Chem.* **1980**, *35,* 1341.
[9] D. Kussmann, R.-D. Hoffmann, R. Z. Pöttgen, *Anorg. Allg. Chem.* **1998**, *624,* 1727.
[10] A. E. Dwight, *Proc. 12th Rare Earth Res. Conf.*, 1976, Vol. 1, 480.
[11] U. Zachwieja, *Z. Anorg. Allg. Chem.* **2001**, *627*, 353.
[12] M. Liu, L.-G. Liu, *High Temp. High Pressures* **1986**, *18*, 79.
[13] E. Jette, F. Foote, *J. Chem. Phys.* **1935**, *3*, 605.
[14] A. Szytula, M. Hofmann, J. Leciejewicz, B. Penc, A. Zygmunt, *J. Alloys Compd.* **2001**, *316*, 58.
[15] M. T. Kelemen, M. S. S. Brooks, E. Dormann, *J. Phys.: Condens. Matter* **2001**, *13*, 657.
[16] W. Bazela, M. Hofmann, S. Baran, B. Penc, A. Szytula, A. Zygmunt, *Acta Phys. Pol., A* **2000**, *97*, 819.

[17] L. Keller, A. Donni, H. Kitazawa, *Physica B* **2000**, *276–278*, 672.
[18] H. Kitazawa, A. Donni, G. Kido, *Physica B* **2000**, *281–282*, 165.
[19] N. Kumar, F. Harish, S. K. Malik, *Solid State Commun.* **2000**, *114*, 223.
[20] F. Canepa, M. Napoletano, A. Palenzona, F. Merlo, S. Cirafici, *J. Phys. D: Appl. Phys.* **1999**, *32*, 2721.
[21] D. Kaczorowski, A. Leithe-Jasper, P. Rogl, H. Flandorfer, T. Cichorek, R. Pietri, B. Andraka, *Phys. Rev. B: Condens. Matter Mater. Phys.* **1999**, *60*, 422.
[22] B. Penc, M. Hofmann, J. Leciejewicz, M. Slaski, A. Szytula, *J. Alloys Compd.* **1999**, *287*, 18.
[23] R. Pöttgen, G. Kotzyba, E. A. Gorlich, K. Latka, R. Dronskowski, *J. Solid State Chem.* **1998**, *141*, 352.
[24] S. Baran, M. Hofmann, J. Leciejewicz, B. Penc, M. Slaski, A. Szytula, *J. Alloys Compd.* **1998**, *281*, 92.
[25] A. Szytula, *Diffus. Defect Data, Pt. B* **1998**, *61–62* (Contemporary Studies in Condensed Matter Physics), 27.
[26] S. Kawano, Y. Andoh, M. Kurisu, *Kidorui* **1998**, *32*, 190.
[27] L. Keller, A. Donni, H. Kitazawa, J. Tang, F. Fauth, M. Zolliker, *Physica B* **1998**, *241–243*, 660.
[28] S. Kawano, Y. Andoh, M. Kurisu, *J. Magn. Magn. Mater.* **1998**, *182*, 393.
[29] A. Dascoulidou, P. Mueller, W. Bronger, *Z. Anorg. Allg. Chem.* **1998**, *624*, 124.
[30] V. Ivanov, A. Szytula, *J. Alloys Compd.* **1997**, *262–263*, 253.
[31] S. Baran, M. Hofmann, J. Leciejewicz, M. Slaski, A. Szytula, A. Zygmunt, *J. Phys.: Condens. Matter* **1997**, *9*, 9053.
[32] R. V. Skolozdra, A. Guzik, A. M. Goryn, *J.* Pierre, *Acta Phys. Pol., A* **1997**, *92*, 343.
[33] A. Szytula, *Liet. Fiz. Z.* **1997**, *37*, 32.
[34] G. Ehlers, H. Maletta, Z. *Phys. B: Condens. Matter* **1996**, *101*, 317.
[35] F. Canepa, P. Manfrinetti, M. Pani, A. Palenzona, *J. Alloys Compd.* **1996**, *234*, 225.
[36] G. Ehlers, H. Maletta, *Phys. B: Condens. Matter* **1996**, *99*, 145.
[37] A. V. Andreev, H. A. Katori, T. Goto, *J. Alloys Compd*. **1995**, *224*, 86.
[38] R. A. Robinson, A. C. Lawson, V. Sechovsky, L. Havela, Y. Kergadallan, H. Nakotte, F. R. de Boer, *J. Alloys Compd.* **1994**, *213–214*, 528.
[39] G. Cordier, T. Friedrich, R. Henseleit, A. Grauel, U. Tegel, C. Schank, C. Geibel, *J. Alloys Compd.* **1993**, *201*, 197.
[40] S. K. Malik, H. Takeya, K. A. Gschneidner, *Phys. Rev. B: Condens. Matter* **1993**, *48*, 9858.
[41] M. Kasaya, H. Suzuki, K. Katoh, M. Inoue, T. Yamaguchi, *JJAP Ser.* **1993**, *8* (Physical Properties of Actinide and Rare Earth Compounds), 223.
[42] P. Bonville, P. Bellot, J. A. Hodges, P. Imbert, G. Jehanno, G. Le Bras, J. Hammann, L. Leylekian, G. Chevrier, *Physica B* **1992**, *182*, 105.
[43] J. H. V. J. Brabers, F. R. De Boer, K. H. J. Buschow, *J. Alloys Compd.* **1992**, *179*, 227.
[44] V. H. Tran, R. Troc, *J. Magn. Magn. Mater.* **1991**, *102*, 74.
[45] F. Yang, J. P. Kuang, J. Li, E. Bruck, H. Nakotte, F. R. De Boer, X. Wu, Z. Li, Y. Wang, *J. Appl. Phys.* **1991**, *69*, 4705.
[46] M. Zeleny, *J. Magn. Magn. Mater.* **1991**, *94*, 85.
[47] J. Sakurai, Y. Yamaguchi, S. Nishigori, T. Suzuki, T. Fujita, *J. Magn. Magn. Mater.* **1990**, *90–91*, 422.
[48] M. N. Nyayate, S. H. Devare, S. K. Malik, D. T. Adroja, H. G. Devare, *Phys. Lett. A* **1990**, *151*, 547.
[49] H. Fujii, H. Kawanaka, T. Takabatake, E. Sugiura, K. Sugiyama, M. Date, *J. Magn. Magn. Mater.* **1990**, *87*, 235.
[50] J. Sakurai, Y. Yamaguchi, K. Mibu, T. Shinjo, *J. Magn. Magn. Mater.* **1990**, *84*, 157.
[51] F. R. De Boer, E. Bruck, A. A. Menovsky, P. A. Veenhuizen, V. Sechovsky, L. Havela, K. H. Buschow, *J. Physica B* **1989**, *155*, 221.
[52] L. Havela, V. Sechovsky, F. R. De Boer, E. Brueck, P. A. Veenhuizen, J. B. Bouwer, K. H. J. Buschow, *J. Magn. Magn. Mater.* **1988**, *76–77*, 89.
[53] A. H. El-Sayed, G. J. Nieuwenhuys, J. A. Mydosh, K. H. J. Buschow, *J. Phys. F: Met. Phys.* **1988**, *18*, 2265.
[54] F. G. Aliev, N. B. Brandt, V. V. Kozyr'kov, V. V. Moshchalkov, R. V. Skolozdra, Yu. V. Stadnik, *Fiz. Nizk. Temp. (Kiev)* **1987**, *13*, 498.
[55] L. Havela, L. Neuzil, V. Sechovsky, A. V. Andreev, C. Schmitzer, G. Hilscher, *J. Magn. Magn. Mater.* **1986**, *54–57*, 551.
[56] K. H. J. Buschow, D. B. De Mooij, T. T. M. Palstra, G. J. Nieuwenhuys, J. A. Mydosh, *Philips J. Res.* **1985**, *40*, 313.
[57] L. Havela, J. Hrebik, M. Zeleny, A. V. Andreev, *Acta Phys. Pol., A* **1985**, *68*, 493.
[58] M. Maple, *Physica B* **1995**, *215*, 110.

[59] F. Hulliger, *J. Alloys Compd*. **1993**, *196*, 225.
[60] T. T. M. Palstra, G. J. Nieuwenhuys, R. F. M. Vlastuin, J. A. Mydosh, K. H. J. Buschow, *J. Appl. Phys.* **1988**, *63*, 4279.
[61] R. Pöttgen, D. Johrendt, *Chem. Mater.* **2000**, *12,* 875.
[62] L. Havela, V. Sechovsky, *Acta Phys. Slovaca* **1998**, *48*, 797.
[63] T. Gasche, S. Auluck, M. S. S. Brooks, B. Johansson, *J. Magn. Magn. Mater.* **1992**, *104–107* (Proc. Int. Conf. Magn. **1991**, Pt. 1), 37.
[64] Y. Tagawa, K. Inaba, J. Sakurai, Y. Komura, *Solid State Commun.* **1988**, *66*, 993.
[65] V. Sechovsky, L. Havela, F. R. De Boer, J. J. M. Franse, P. A. Veenhuizen, J. Sebek, J. Stehno, A. V. Andreev, *Physica B–C* **1986**, *142*, 283.
[66] J. Evers, G. Oehlinger, K. Polborn, B. Sendlinger, *J. Solid State Chem.* **1993**, *103*, 45.
[67] J. Evers, G. Oehlinger, *J. Solid State Chem.* **1986**, *62*, 133.
[68] G. LeBras, P. Bonville, J. A. Hodges, J. Hammann, M. J. Besnus, G. Schmerber, S. K. Dhar, F. G. Aliev, G. Andre, *J. Phys.: Condens. Matter* **1995**, *7*, 5665.
[69] H. Fujii, T. Takabatake, Y. Andoh, *J. Alloys Compd.* **1992**, *181*, 111.
[70] D. Kussmann, R. Pöttgen, B. Kuennen, G. Kotzyba, R. Muellmann, B. D. Z. Mosel, *Kristallogr.* **1998**, *213*, 356.
[71] V. A. Yartys, T. Olavesen, B. C. Hauback, H. Fjellvag, H. W. Brinks, *J. Alloys Compd.* **2002**, *330–332*, 141.
[72] S. K. Malik, P. Raj, A. Sathyamoorthy, K. Shashikala, N. H. Kumar, L. Menon, *Phys. Rev. B: Condens. Matter* **2001**, *63*, 172418.
[73] P. Raj, A. Sathyamoorthy, K. Shashikala, C. R. V. Rao, S. K. Malik, *Solid State Commun.* **2001**, *120*, 375.
[74] V. A. Yartys, R. V. Denys, B. C. Hauback, H. Fjellvag, I. I. Bulyk, A. B. Riabov, Ya. M. Kalychak, *J. Alloys Compd.* **2002**, *330–332*, 132.
[75] A. V. Kolomiets, L. Havela, V. A. Yartys, A. V. Andreev, *Zh. Fiz. Dosl.* **1999**, *3*, 55.
[76] A. V. Kolomiets, L. Havela, V. A. Yartys, A. V Andreev, *J. Alloys Compd.* **1997**, *253–254*, 343.
[77] J. H. Albering, R. Pöttgen, W. Jeitschko, R. D. Hoffmann, B. Chevalier, J. Etourneau, *J. Alloys Compd.* **1994**, *206*, 133.
[78] A. Slebarski, E. D. Bauer, S. Li, M. B. Maple, A. Jezierski, *Phys. Rev. B: Condens. Matter Mater. Phys.* **2001**, *63*, 125126-1.
[79] F. Merlo, M. Pani, M. L. Fornasini, *J. Less-Common Met.* **1991**, *171*, 329.
[80] F. Merlo, M. Pani, M. L. Fornasini, *J. Less-Common Met.* **1990**, *166*, 319.
[81] M. Martinez-Ripoll, A. Haase, G. Brauer, *Acta Crystallogr, Sect. B* **1974**, *30*, 2003.
[82] B. Eisenmann, K. Deller, *Z. Naturforsch., Teil B* **1975**, *30*, 66.
[83] N. N. Zhuravlev, V. P. Melik-Adamyan, *Sov. Phys. Crystallogr.* **1961**, *6*, 99.
[84] C. B. Shoemaker, D. P. Shoemaker, *Acta Crystallogr.* **1965**, *18*, 900.
[85] S. P. Alisova, Yu. K. Kovneristyi, Yu. E. Lazareva, P. B. Budberg, *Izv. Akad. Nauk SSSR, Met.* **1991**, *1*, 219.
[86] B. Penc, M. Hofmann, M. Slaski, A. Szytula, A. Zygmunt, *Physica B* **2000**, *291*, 19.
[87] V. I. Zaremba, Y. V. Galadzhun, B. D. Belan, A. Pikul, J. Stepien-Damm, D. Kaczorowski, *J. Alloys Compd.* **2001**, *316*, 64.
[88] G. Nuspl, K. Polborn, J. Evers, G. A. Landrum, R. Hoffmann, *Inorg. Chem.* **1996**, *35*, 6922.
[89] G. A. Landrum, R. Hoffmann, J. Evers, H. Boysen, *Inorg. Chem.* **1998**, *37*, 5754.
[90] R. Pöttgen, *Z. Naturforsch., B: Chem. Sci.* **1995**, *50*, 1071.
[91] Y. M. Prots, R. Pöttgen, D. Niepmann, M. W. Wolff, W. Jeitschko, *J. Solid State Chem.* **1999**, *142*, 400.
[92] A. C. Larson, *Acta Crystallogr.* **1961**, *14*, 73.
[93] E. J. Duwell, N. C. Baenziger, *Acta Crystallogr.* **1955**, *8*, 705.
[94] F. Merlo, M. Pani, M. L. Fornasini, *J. Alloys Compd.* **1996**, *232*, 289.
[95] R. Pöttgen, *J. Alloys Compd.* **1996**, *243*, L1.
[96] R. Mullmann, U. Ernet, B. D. Mosel, H. Eckert, R. K. Kremer, R.-D. Hoffmann, R. Pöttgen, *J. Mater. Chem.* **2001**, *11*, 1133.
[97] R. Pöttgen, G. Kotzyba, F. M. Schappacher, B. D. Mosel, H. Eckert, Y. Grin, *Z. Anorg. Allg. Chem.* **2001**, *627*, 1299.
[98] D. Mazzone, D. Rossi, R. Marazza, R. Ferro, *J. Less-Common Met.* **1981**, *80,* P47.
[99] F. Merlo, M. Pani, M. L. Fornasini, *J. Alloys Compd.* **1996**, *232*, 289.
[100] D. Kaczorowski, A. Leithe-Jasper, P. Rogl, H. Flandorfer, T. Cichorek, R. Pietri, B. Andraka, *Phys. Rev. B: Condens. Matter Mater. Phys.* **1999**, *60*, 422.
[101] K. Katoh, T. Takabatake, A. Minami, I. Oguro, H. Sawa, *J. Alloys Compd.* **1997**, *261*, 32.

[102] R. Pöttgen, P. E. Arpe, C. Felser, D. Kuszmann, R. Mullmann, B. D. Mosel, B. Kunnen, G. Kotzyba, *J. Solid State Chem.* **1999**, *145*, 668.
[103] G. Zanicchi, D. Mazzone, P. Riani, R. Marazza, R. Ferro, *J. Alloys Compd.* **2001**, *317–318*, 513.
[104] R. Pöttgen, B. Gibson, R. K. Kremer, *Z. Kristallogr.* **1997**, *212*, 58; V. I. Zaremba, Y. M. Kalychak, V. P. Dubenskiy, R.-D. Hoffmann, R. Pöttgen, *J. Solid State Chem.* **2000**, *152*, 560.

Received March 10, 2003